Lithos 284–285 (2017) 109–121

Contents lists available at ScienceDirect

Lithos

journal homepage: www.elsevier.com/locate/lithos

A felsic MASH zone of crustal magmas — Feedback between granite magma intrusion and *in situ* crustal anatexis

Martin Schwindinger *, Roberto F. Weinberg

School of Earth, Atmosphere and Environment, Monash University, Clayton, VIC 3800, Australia

ARTICLE INFO

Article history:
Received 14 December 2016
Accepted 29 March 2017
Available online 08 April 2017

Keywords:
Migmatite
Granite
MASH
Magma-mixing
Water-fluxed melting

ABSTRACT

Magma mixing and mingling are described from different tectonic environments and are key mechanisms in the evolution of granitoids. The literature focuses on the interaction between mafic and felsic magmas with only limited research on the interaction between similar magmas. Here, we investigate instead hybridization processes between felsic magmas formed during the ~500 Ma Delamerian Orogeny on the south coast of Kangaroo Island. Field relations suggest that a coarse, megacrystic granite intruded and interacted with a fine-grained diatexite that resulted from combined muscovite dehydration and water-fluxed melting of Kanmantoo Group turbidites. The two magmas hybridized during syn-magmatic deformation, explaining the complexity of relationships and variability of granitoids exposed. We suggest that granite intrusion enhanced melting of the turbidites by bringing in heat and H_2O. With rising melt fraction, intrusive magmas became increasingly unable to traverse the partially molten terrane, creating a positive feedback between intrusion and anatexis. This feedback loop generated the exposed mid-crustal zone where magmas mixed and homogenized. Thus, the outcrops on Kangaroo Island represent a crustal and felsic melting-assimilation-storage-homogenization (felsic MASH) zone where, instead of having direct mantle magma involvement, as originally proposed, these processes developed in a purely crustal environment formed by felsic magmas.

1. Introduction

The production of granitic magmas by partial melting of metamorphic rocks and their consequent rise in the continental crust is one of the fundamental mechanisms in the evolution of the Earth and the main driver of crustal differentiation (Brown, 2013; Sawyer et al., 2011). To understand the nature of magmas that incrementally feed upper crustal plutons, it is necessary to investigate all stages of this process, from the sources of granite magmas to the pathways that link to the top. This includes the initial steps of melt generation in a heterogeneous crust (Patiño Douce and Harris, 1998; Stevens et al., 1997; Weinberg and Hasalová, 2015), the mechanism of melt extraction and ascent (Vanderhaeghe, 2001; Weinberg and Regenauer-Lieb, 2010), interactions between magma and their surroundings during ascent, and processes related to accumulation within subsolidus crust (Diener et al., 2014; Hall and Kisters, 2016). It is the superposition and temporal variation of these different processes that gives granite plutons their distinct character (Clemens and Stevens, 2012).

Because exposure of continuous granitic systems from migmatite sources in the lower crust to upper crustal granite plutons is rare (see Reichardt and Weinberg, 2012a), our current knowledge is based on integrating studies of different parts of this system. Due to a number of seminal papers in the 1980s, water-absent dehydration melting of crustal rocks at granulite facies metamorphism has been commonly seen as the most efficient producer of granitic magmas contributing to form large plutons (*e.g.* Patiño Douce and Johnston, 1991; Yakymchuk and Brown, 2014). However, water-fluxed melting has also been shown to be of regional importance, with voluminous melt production at upper amphibolite facies conditions, underlining its contribution to granite magmatism (Carvalho et al., 2016; Collins et al., 2016; Weinberg and Hasalová, 2015). Regardless of protolith and melt reaction, anatectic melt is likely to be modified before its final emplacement by mechanisms such as crystal fractionation (Carvalho et al., 2016), entrainment of residual (Chappel et al., 1987) and peritectic phases (Reichardt and Weinberg, 2012b; Stevens et al., 2007) or magma mixing (Gray and Kemp, 2009; Keay et al., 1997).

The significance of magma mixing in the evolution of granitic magmas remains actively debated (Regmi et al., 2016). While many authors consider magma mixing as a leading process in granite petrogenesis (*e.g.* Collins, 1996; Regmi et al., 2016), some regard it as a late, shallow crustal feature, without any significance for the large-scale geochemical variety of granite magmas (Clemens and Stevens, 2012). Eye-catching features of magma mingling, with dispersion of dark-coloured magmas in a more leucocratic host, are taken by many geologists as typical features of magma mixing. This interpretation is

* Corresponding author.
E-mail address: martin.schwindinger@monash.edu (M. Schwindinger).

http://dx.doi.org/10.1016/j.lithos.2017.03.030
0024-4937/

generally supported by a hybrid isotopic signature indicative of mixing (Foden et al., 2002; Waight et al., 2000). Common arguments against mixing are based on inconsistencies in mixing arrays between major, trace element and isotope ratios (Clemens and Stevens, 2012; Farina et al., 2014). It is suggested instead that source composition is the most significant parameter controlling granite magma composition.

Almost three decades ago Hildreth and Moorbath (1988) proposed that hybridization between crustal and mantle magmas in magmatic arcs occurs in a zone at the base of the continental crust where melting, assimilation, storage and homogenization takes place in what they called MASH zones. In such zones, basaltic mantle magmas cause melting or remelting of lower crustal rocks, with which they hybridize and homogenize before rising and fractionating. Originally envisaged for magmatic arc settings, these hypothetical zones, and the similar deep crustal hot zones (Annen et al., 2006), have been used in numerous publications to explain the mixed isotopic composition of granitoids in all sort of tectonic setting, including the accretionary orogens of eastern Australia (Collins, 1996; Foden et al., 2002).

Criticism of the role of MASH in granite petrogenesis is commonly based on different properties of felsic and mafic magmas and fast melt extraction rates from the source, inhibiting interaction between different magmas. In addition there seems to be a lack of examples of such zones in the geologic record (Clemens and Stevens, 2016). Experiments showed that the efficiency of magma hybridization is strongly dependent on the rheology of the participating magmas, as well as their solidus temperatures and relative density contrasts, with most homogeneous hybrids resulting from mixing of similar end-member magmas (Perugini and Poli, 2012; Sparks and Marshall, 1986). Despite these physical difficulties, most studies have focused on the interaction between a felsic crustal magma and a mafic, mantle-derived magma, whereas the hybridization between magmas of similar composition has attracted less attention, with only a few examples in the literature, all of which in migmatites (Hasalova et al., 2011; Reichardt et al., 2010; Weber and Barbey, 1986). However, it is precisely that these magmas may interact efficiently.

This paper addresses hybridization of magmas with similar composition by describing the hybridization processes between intrusive granitic magmas and migmatites preserved in exposures on the south coast of Kangaroo Island (Foden et al., 2002; Weinberg et al., 2013). We start the paper with a brief summary of the regional geology, followed by a description of the different lithologies involved, and then investigate their patterns of interaction, from which we infer a series of processes that gave rise to a felsic MASH zone formed entirely by crustal magmas.

2. Regional geology

Kangaroo Island is located at the most westerly extension of the arcuate Adelaide Fold Belt, which was deformed during the Cambro-Ordovician Delamerian Orogeny (514–490 Ma, Foden et al., 2006). The belt hosts deformed sedimentary successions ranging in depositional age from Late Neoproterozoic to Early Cambrian, terminating with the deposition of the Cambrian Kanmantoo Group as the youngest stratigraphic member. This group comprises a thick marine succession of immature turbiditic sand- and mudstones with wide exposure in the southern Adelaide Fold Belt (Fig. 1, Flöttmann et al., 1998). The Kanmantoo Group hosts multiple felsic, igneous intrusions of the Delamerian Orogen and is the protolith for the migmatites studied here (Foden et al., 2002; Weinberg et al., 2013). On Kangaroo Island these are exposed south of the Kangaroo Island Shear Zone, a regional structure which divides the island into two tectonostratigraphic units: the unmetamorphosed platformal Kangaroo Island Group to the north, and the deformed and metamorphosed Kanmantoo Group sedimentary rocks to the south (Fig. 1).

Delamerian crustal shortening commenced only ~8 m yr after the onset of the Kanmantoo Group deposition at 522 Ma (Jenkins et al., 2002) and included intense deformation and metamorphism of the

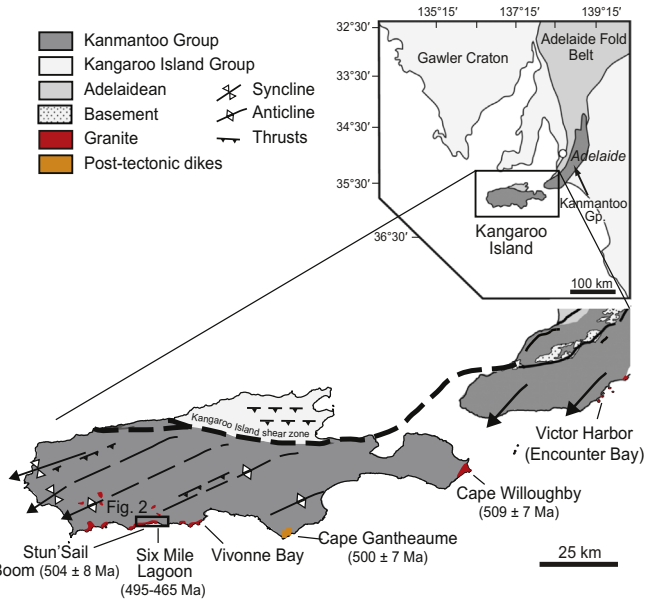

Fig. 1. Position of Kangaroo Island in the southern Adelaide Fold Belt showing the extent of the Kanmantoo Group, the location of syntectonic granites and geological features mentioned in the text. Granite intrusions between Stun'Sail Boom and Vivonne Bay are surrounded by migmatite. Other granites are intruded into shallower crustal levels, such as Cape Willoughby and Encounter Bay Granites. All ages are SHRIMP zircon ages (Fanning, 1990) except for SHRIMP monazite ages from Six Mile Lagoon migmatites (Weinberg et al., 2013). The study area is marked by a black rectangle. Map modified after data from Foden et al. (2006), Mancktelow (1990) and Weinberg et al. (2013).

turbiditic sequences (Foden et al., 2006; Mancktelow, 1990), forming what is now the Adelaide Fold Belt. Estimates for the beginning of deformation vary from the appearance of first syntectonic granites at 514 ± 4 Ma (Foden et al., 1999), to an earlier Neoproterozoic onset of Delamerian deformation (547–544 Ma, Turner et al., 2009). During low-pressure-high-temperature "Buchan-style" metamorphism, peak conditions reached 4–4.5 kbar at 650 °C (Dymoke and Sandiford, 1992), with highest metamorphic grades associated with migmatites in the vicinity of several granite intrusions (Sandiford et al., 1992). This relationship is also observed in the area covered by this study between Stun'Sail Boom River and Vivonne Bay (Fig. 1). Here the Kanmantoo Group has been intruded by several syn-tectonic, I-S type granites (503 ± 4 Ma, 504 ± 8 Ma; Fanning, 1990) and undergone partial melting forming migmatites (Foden et al., 2002; Weinberg et al., 2013).

These syn-tectonic Delamerian granites are interpreted to be the result of multi-stage mixing between mantle-derived mafic magmas and crustal material at deep crustal levels, with S-type granites being representative of magmas that are derived from melting of the Cambrian sediments (Foden et al., 2002). *In situ* melting of meta-sedimentary rocks to form migmatite has been inferred to be the product of muscovite dehydration melting, which is indicated by the local presence of sillimanite (Tassone, 2008). Higher metamorphic conditions exceeding the stability field of biotite are unlikely, because biotite appears stable and ferromagnesian peritectic minerals are absent.

Weinberg et al. (2013) investigated the role of deformation in the extraction of magmas from migmatites and defined four syn-magmatic deformation phases, which only partly correlate to the regional deformation phases recorded in lower grade rocks of the orogen (Mancktelow, 1990). The syn-magmatic deformation was subdivided into compressional phases, in which melt migrated along fold limbs into axial-planar dikes, and transtensional deformation phases characterized by melt accumulation on shear planes and formation of diatexites. U–Pb SHRIMP dating of monazite from the diatexites at Six Mile Lagoon indicate protracted syn-tectonic anatexis between 495 and 465 Ma (Weinberg et al., 2013). This result extends the age range

to younger values when compared to results from monazite extracted from leucosomes (498–488 Ma, Tassone, 2008). These ranges are apparently contradicted by a Rb–Sr cooling age of an intrusive leucogranite further east at Vivonne Bay (487.4 ± 3.5 Ma, Foden et al., 2002) and the 500 ± 7 Ma zircon ages of composite dikes at Cape Gantheaume (Fig. 1, Fanning, 1990), that were interpreted to be related to a regional post-convergent extensional phase. A resolution to this apparent contradiction may lie in different exposure crustal and the nature and uncertainties of the different dating methods. It is also possible that low-T melting in the Kanmantoo Group continued into the extensional stage of the orogen (Foden et al., 2006). This stage was associated with a renewed influx of hot mantle, and transition from convergent to extensional tectonics was accompanied by a compositional shift to bimodal magmatism and A-type granite intrusions (493–480 Ma), and terminates the Delamerian Orogeny (summarized in Foden et al., 2006).

3. Results

Fig. 2 presents the geological map of the Stun'Sail Boom area and photographs of the most common lithologies. The outcrops are subdivided into three broad zones (Fig. 2a). Schollen-rich diatexite in the west, diatexite with variable proportions of megacrystic granite intrusions (20–40 vol.% by area) in the centre, and metatexite in the east. The lithological boundaries, in particular between diatexite and megacrystic granite in the central zone, vary from well-defined to diffuse, and from planar to strongly irregular. We will first describe the main rock types in order of increasing former melt content from

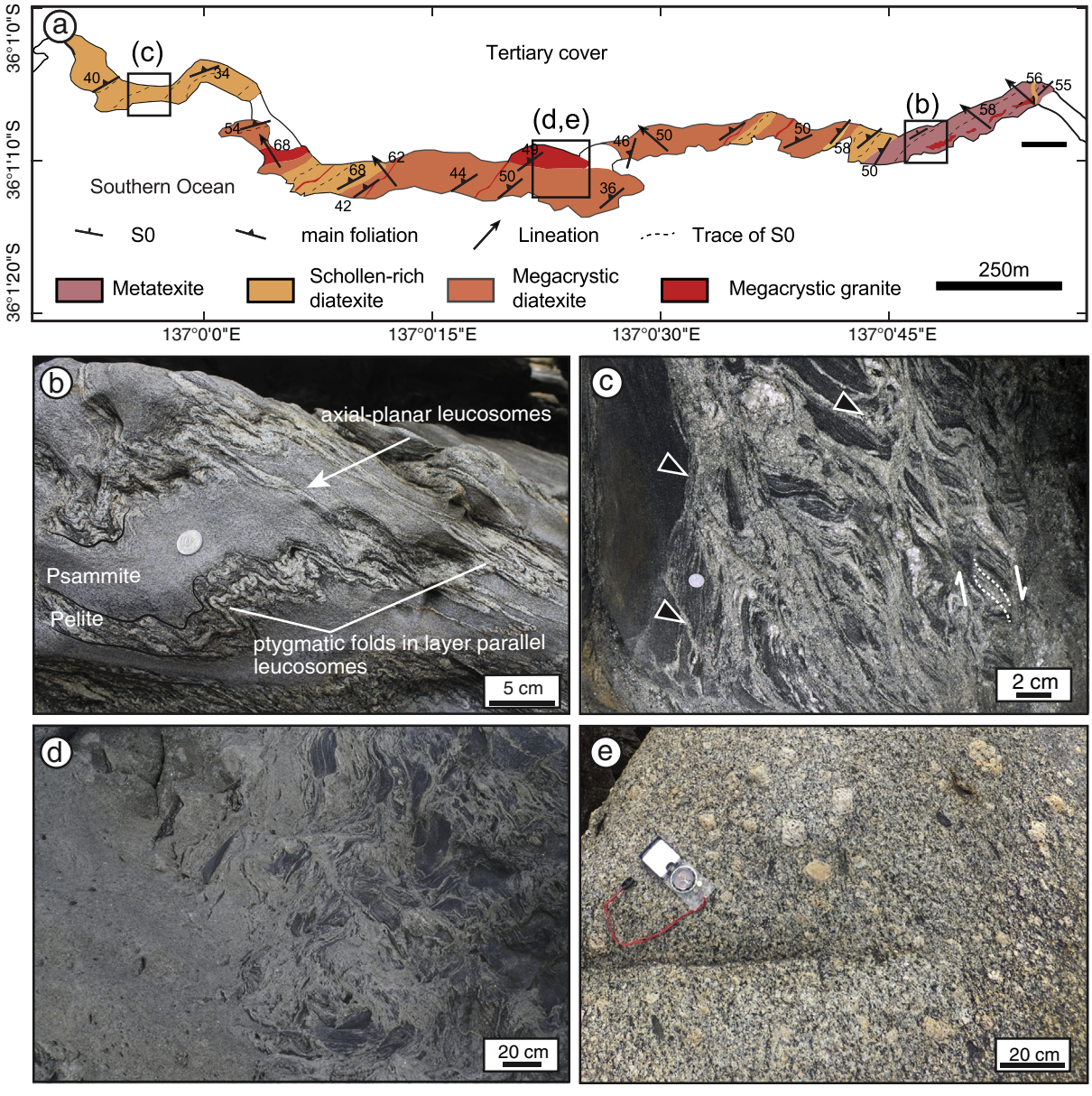

Fig. 2. Geological map and main rock types in the Stun'Sail Boom River area. (a) Simplified geological map of the distribution of main rock types. The most voluminous lithology is diatexite and is associated with variable proportions of intrusive granite. Small rectangles show the location of the photographs in (b) to (e). (b) Partially melted Kanmantoo metasedimentary rocks forming a metatexite. Feldspathic psammite alternates with biotite-rich pelite layers. Layer-parallel leucosomes are more voluminous in pelite and ptygmatically folded. A second set of leucosomes crosscut bedding, parallel to axial planar orientation of folds, creating an interconnected network of leucosomes. (c) Diatexite loaded with biotite-rich schollen, clots and schlieren representing physical disaggregation of metatexite. Leucosomes in the diatexite are linked continuously with layer-parallel leucosomes in schollen (black arrows), suggesting increase in melt proportion by both *in-situ* melting and channelling of *in source* melting products. Asymmetries in the orientation of the clasts and schlieren indicate dextral shearing (photograph of a horizontal plane). (d) Transition from schollen-rich diatexite to cleaner, grey diatexite with small (<10 cm) biotite clots. (e) Intrusive, megacrystic granite. They are more leucocratic and coarser than diatexitic granites (*e.g.* in Panel c), and have foliation defined by alignment of biotite, inclusion-rich K-feldspar megacrysts and small mafic clots.

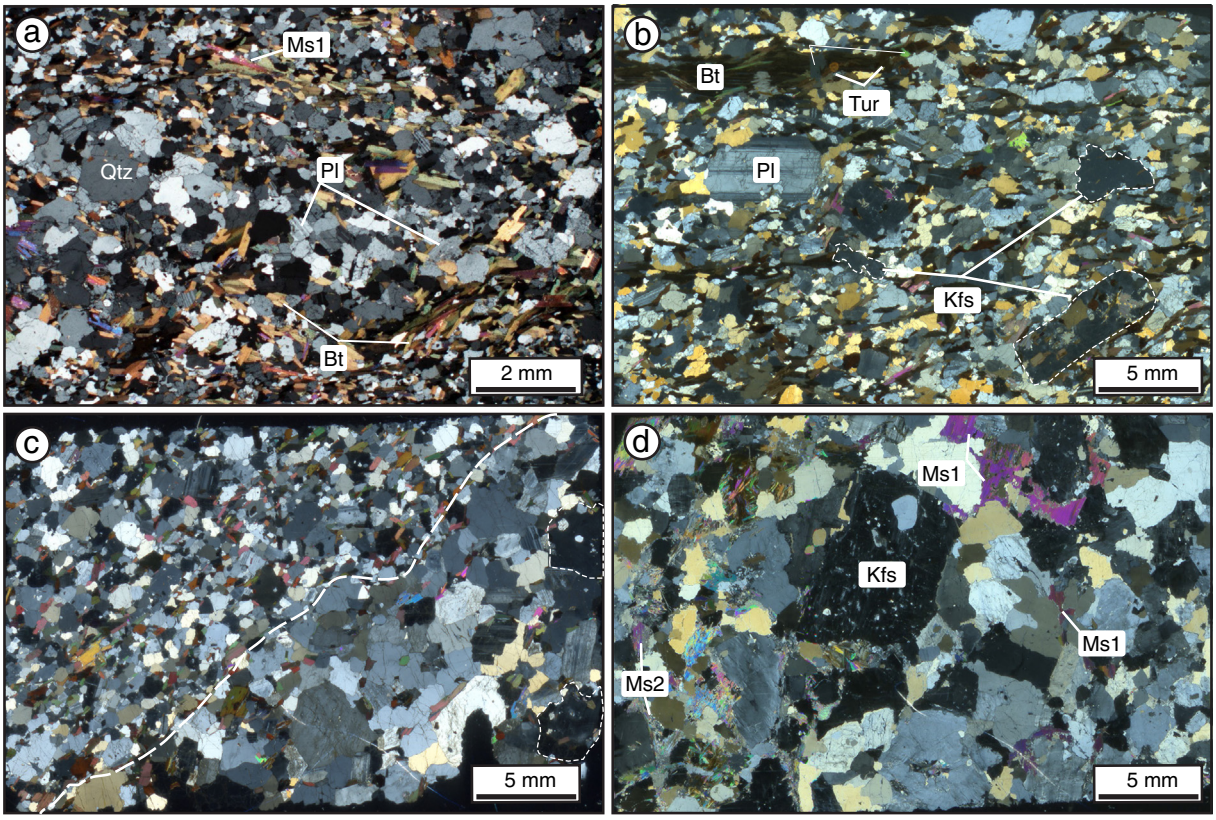

Fig. 3. Photomicrographs of the most common rock types. (a) Metatexite migmatite formed by partial melting of biotite-rich psammite. The leucosome in the centre consists of coarse-grained plagioclase and quartz and has diffuse margins to the surrounding finer-grained residual metasedimentary rock. Type 1 muscovite (Ms1) represents early metamorphic grains, is associated with biotite and both define foliation. (b) Diatexite with single and clotted biotite grains defining foliation. Matrix contains larger plagioclase phenocrysts and anhedral K-feldspar crystals. From left to right, dashed lines mark interstitial, irregular and an inclusions-rich, K-feldspar phenocryst. The latter is similar to the ones in intrusive granite. (c) Contact between coarse-grained megacrystic granite (right-hand side) and finer-grained, biotite rich diatexite (left-hand side) defining an irregular contact diagonally through the photomicrograph. Note inclusion-rich K-feldspar crystals in the granite delineated by dashed lines. (d) Leucogranite, with coarse grainsize and irregular muscovite interstitial between quartz and K-feldspar, interpreted to have crystallized from a magma close to the solidus conditions (Ms1). Small, irregular muscovite flakes appear to replace K-feldspar and are likely of secondary origin (Ms2). Note the quartz inclusions in the K-feldspar in the centre of the photomicrograph.

metatexite to intrusive granites (Figs. 2–4), followed by a description of contact relationships (Figs. 5–9). We use the term leucosome to refer to magmatic segregations interpreted to be originated *in situ*, and granite intrusions to refer to externally-derived magmas that invaded the migmatites.

Fig. 4. Composite enclave within megacrystic granite comprising a layered metasedimentary enclave in the core surrounded by a rim of coarse-grained, foliated gneissic granite (dashed line outlines parts of the margin). A thin gneissic rim is present around the K-feldspar megacryst at the bottom left of the photograph. Except for the gneissic foliation, the granite in the composite enclave is texturally and modally similar to the surrounding coarse-grained granite suggesting erosion of a pre-existing granite formed during the same anatexis.

3.1. Lithologies

3.1.1. Metatexite

Metatexite retains pre-melting structures and consists of alternating bands of grey feldspathic psammites and black biotite-rich pelite layers, with indication of *in situ* melt generation (Fig. 2b). The psammite layers are dominated by quartz (30–38 vol.%), plagioclase (~25 vol.%) and biotite (24–28 vol.%) with minor or absent K-feldspar (0–5 vol.%), whereas in the pelite, biotite makes up to 40 vol.% next to plagioclase, quartz with minor muscovite and K-feldspar (<5 vol.%). The modal abundance of muscovite is small typically <3 vol.%, reaching a maximum of 5 vol.%. Two types of muscovite are distinguished. Type 1 muscovite is fine-grained and associated with biotite with both minerals defining the foliation of the rock. Type 2 muscovite form flakes (<1 cm) with random orientation and irregular spacing between crystals. This coarse muscovite has rare fibrous sillimanite inclusions, restricted to patch or stromatic leucosomes and mica-rich zones in the surrounding of late pegmatite intrusions. Accessory phases in the metatexite are monazite, zircon, apatite, and ilmenite that are commonly associated with biotite. The leucosomes comprise quartz, plagioclase, biotite, minor muscovite and variable amounts of K-feldspar, reflecting a compositional variation from tonalite (more common) to granite (Fig. 3a). These leucosomes are less than 2 cm wide and either parallel to bedding or to the axial-planar orientation of folds, forming stromatic and network metatexite

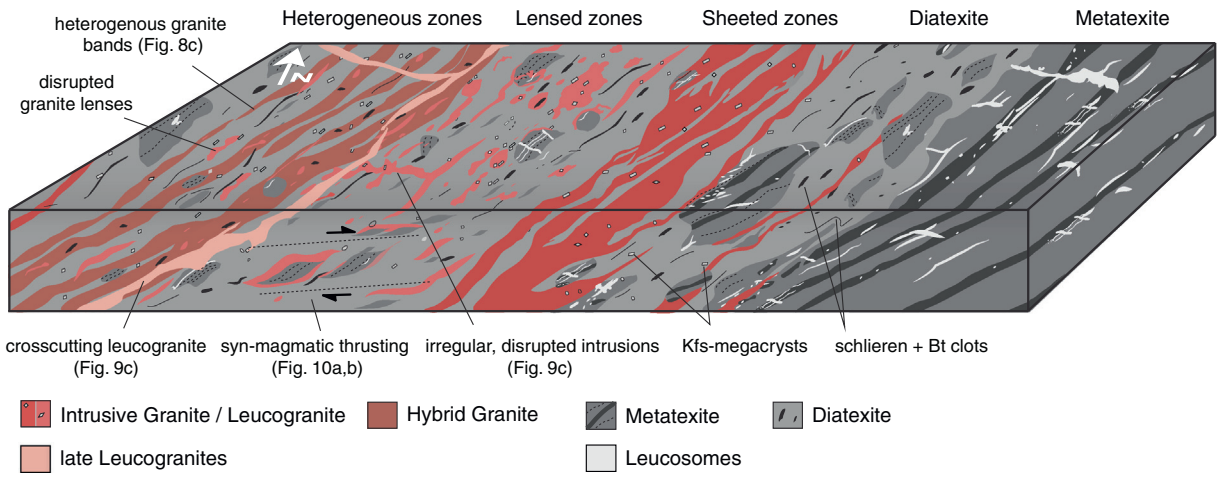

Fig. 5. Schematic block diagram summarizing zones defined by different degrees of interaction between megacrystic intrusive sheets and diatexite/metatexite. The evolution from metatexite to the heterogeneous zone is accompanied by an increase in melt fraction and gradually more intense hybridization from the right- to the left-hand side of the diagram.

(Fig. 2b). With an increase in the total melt fraction in the rock, the metatexite disaggregates to form diatexite migmatite (Fig. 2c).

3.1.2. Diatexite

The most characteristic features of diatexites are their grey colour, fine- to medium grainsize and dispersed remnants of disaggregated metasedimentary rocks. They are compositionally heterogeneous being dominated by a granitic matrix with numerous centimetre to metre-sized Kanmantoo Group schollen, schlieren and biotite clots (Fig. 2c). The proportions of these mafic elements are variable and outcrops range from schollen-and-schlieren diatexites to homogenous, grey diatexitic granites with only few small remnants (Fig. 2c–d).

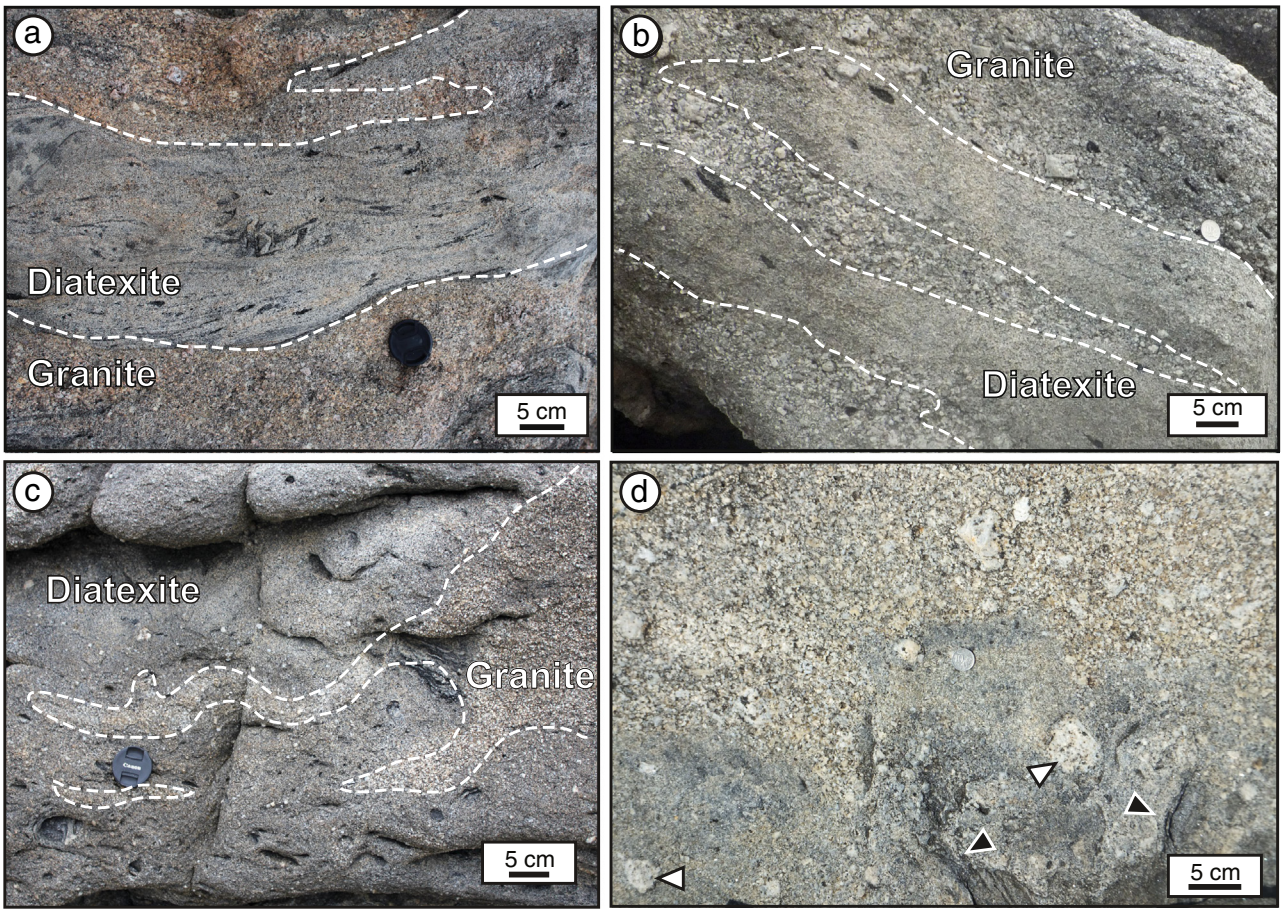

Fig. 6. Clean, sheeted contacts between grey diatexite with stretched schlieren and elongated small schollen, and coarser-grained megacrystic granite (dashed lines). Single sheets of diatexite or megacrystic granite are continuous over up to 8 m with semi-planar, yet irregular contacts and only minor signs of interaction between the two (a,b). Other contacts have increased irregularities and incipient magma interaction (c,d). Note in (b) that the foliation defined by alignment of Kfs megacrysts, biotite clots and elongated schollen, is parallel to sheet contact. In (d) K-feldspar megacrysts from granite are found in diatexite (white arrows) across a crenulated and diffuse contact. Black arrows show biotite-schlieren and schollen fragments.

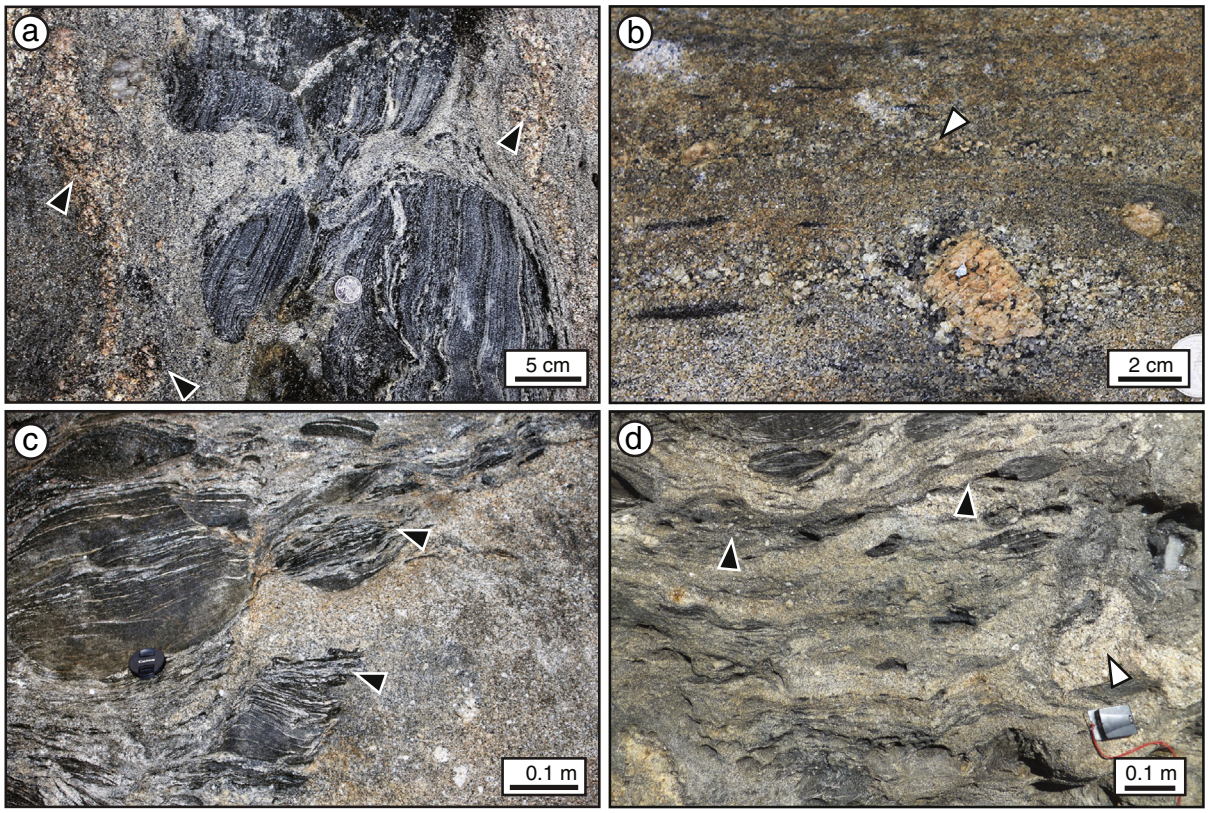

Fig. 7. Increasingly heterogeneous hybrid rocks characterized by disrupted lenses and transitional contact zones. (a) Irregular, disrupted bands of megacrystic granitite (black arrows) inside fine-grained, grey diatexite with schollen. (b) Single Kfs-megacryst in the centre of a sigma-shaped lens of coarse granite forming wings, inside fine-grained, heterogeneous granite. Note several, cm-wide bands of coarser matrix typical of the megacrystic granite (white arrow) and biotite-schlieren typical of the diatexite. (c) Megacrystic granite on right-hand side intruding into schollen-rich diatexite along schollen margins. The intrusion process was frozen in the process of transferring a schollen from diatexite to megacrystic granite suggesting coeval anatexis and intrusion. Leucosomes in schollen are in petrographic continuity with the outside diatexitic magma (left-hand side of the image). (d) Pervasive, foliation-parallel intrusion of megacrystic granite into diatexite with diffuse contacts. Best preserved end-member magmas are found in tails connected to schollen (black arrows) or disrupted lenses of granite (white arrow).

Phenocrysts are rare and the granitic matrix consists of quartz, plagioclase, K-feldspar, biotite, muscovite and accessory tourmaline, zircon and monazite (Fig. 3b, c). Similar to metatexite, coarse-grained, type 2 muscovite forms scattered and randomly oriented grains that cut the foliation defined by the alignment of biotite-schlieren and clots. These can have modal abundances of <3 vol.%.

3.1.3. Intrusive megacrystic granite

The migmatites are intruded by multiple phases of granite from metre-sized dikes and sills to large stocks covering several hundred metres of coastal outcrop (Figs. 1–2). They comprise medium- to coarse-grained biotite granites with rounded to rectangular or square K-feldspar megacrysts of 5–10 cm diameter (Fig. 2e). Megacrysts are rich in inclusion that form concentric rings or irregular clusters of euhedral to sub-rounded grains of biotite and plagioclase, which are associated with irregular films of quartz and muscovite. Beyond quartz and feldspars, the granites are made of 10–14 vol.% biotite, muscovite (<2 vol.%), and accessory monazite, zircon and magnetite (Fig. 3c).

An earlier phase of megacrystic granite is subtly different from the main one: it has slightly coarser grainsize and a more marked foliation defined by the alignment of coarse biotite, resulting in a gneissic appearance. This “gneissic granite” can form continuous regions with irregular contact with the megacrystic granite or form metre-sized rounded to irregular enclaves within the megacrystic granite. Many of these enclaves are composite, with a block of metasedimentary rock in their centre, suggesting that these formed a rigid core that protected the gneissic rim from physical abrasion during its breakdown to form the enclaves (Fig. 4) in the younger granite. This gneissic rim is also present as narrow rims around some of megacrysts in the younger granite.

Both the early, foliated and the younger, unfoliated megacrystic granites have rectangular to rounded xenoliths of typical Kanmantoo Group rocks, and a small number of rounded quartz-diorite enclaves. The latter have a magmatic texture and comprise large, euhedral plagioclase phenocrysts in a groundmass of plagioclase, quartz, biotite, K-feldspar, hornblende with accessory magnetite, ilmenite, titanite, monazite and zircon. Transfer of K-feldspar across the boundaries suggests mingling between the magmatic enclaves and their hosts, which is also reported from other intrusions in the Adelaide Fold Belt, such as the Encounter Bay Granite at higher crustal levels (Fig. 1, Foden et al., 1990).

3.1.4. Leucogranite

Leucogranites intruded migmatites and range from cm- to m-wide dikes and sills. They have medium to coarse grainsize and comprise quartz, K-feldspar and 3–5% of primary muscovite (Fig. 3d). Larger bodies outcrop further east in the Vivonne Bay area (Fig. 1) and are assembled by multiple 20–50 cm wide magma sheets with intergrown patches of tourmaline or garnet with quartz. In contrast to the K-feldspar megacrysts of the intrusive granites, K-feldspar in the leucogranites has few inclusions, typically only quartz (Fig. 3d).

3.2. Field relationships

The distribution and relationships between different magmatic rocks define a number of zones, and their nature hold meaningful information regarding the relative timing and rheology of phases at the time

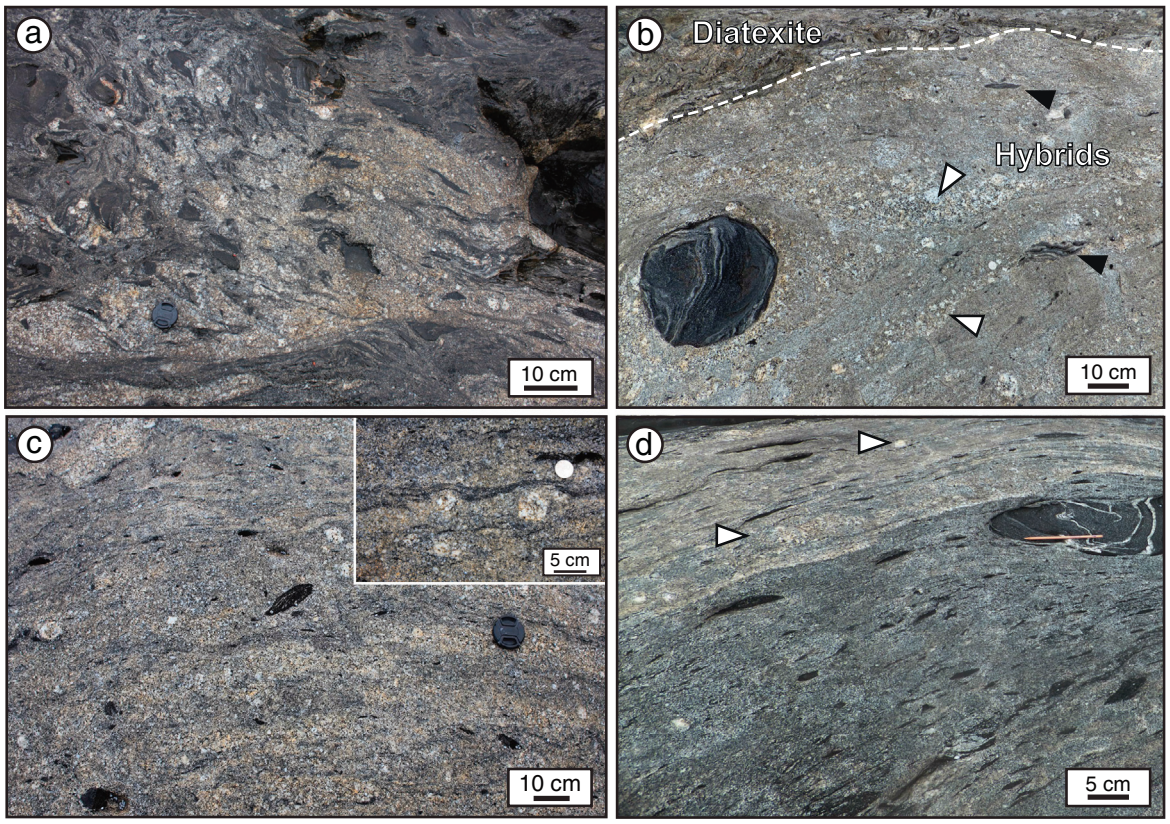

Fig. 8. Advanced mingling between diatexite and megacrystic granite. From (a) to (d) the photographs show increase in homogenization giving rise to a hybrid. (a) Invasion of megacrystic granite from right to left into diatexite, accompanied by a transfer of a swarm of schollen into the granite while stretching the residue-rich interstitial diatexite magma into schlieren. (b) Band of heterogeneous granite in contact with a schollen-rich diatexite. The band comprises irregular regions of fine-grained grey magma with stretched schlieren (black arrows) and schollen typical of diatexite, and disrupted lenses of coarse leucocratic granite and heterogeneously distributed Kfs megacrysts (white arrows) typical of the intrusive granite. (c) Hybrids with varying grey tones and varying amounts of megacrysts and grey schlieren or schollen and diffuse contacts. Inset details hybrid rock showing two megacrysts impinging on a schliere in a matrix of various grey tones. Darker tones are associated with centimetric elongated biotite-clots. (d) Mingling of two strongly foliated diatexites carrying different loads of schollen and coarse leucocratic material. The more leucocratic diatexite with Kfs megacrysts (white arrows) is itself a product of hybridization with megacrystic granite.

of intrusion. We divided the region into sheeted-, lensed- and heterogeneous zones. These are described first, followed by the description of a set of distinct leucogranite and pegmatite dike intrusions (Fig. 5).

3.2.1. Sheeted zones

These are common at the margins of large intrusive granite bodies and are characterized by interleaving between up to 1 m-wide layers of megacrystic granite and fine-grained diatexites (Figs. 5, 6a–b). The difference in grainsize, colour and the presence of megacrysts in one rock and residual source material in the other, creates sharp and planar contacts. Some contacts are more diffuse and have lobated or crenulated to interfingering contacts with minor exchange of solid material across (Fig. 6c–d).

3.2.2. Lensed zones

In lensed zones, the margins are more irregular and diffuse (Fig. 5). A common feature is disrupted sheets of granite and leucogranite that are stretched to irregular lenses of varied sizes inside the diatexite (Fig. 7a–b). Megacrystic granite pervasively intrudes and disaggregates diatexite, which leads to exchange of residual material and K-feldspar megacrysts between them (Fig. 7c–d). Despite the reduction in width and lateral continuity of megacrystic granite and diatexite layers, and the exchange of components between them, the nature of the two magmatic rocks is still recognizable in this zone.

3.2.3. Heterogeneous zones

Here, it becomes difficult to recognize the two end-members and classify them as megacrystic granite or diatexite. Rocks combine a variety of grey tones and typical elements of both end-members (Fig. 8). Megacrystic granites contain schollen, schlieren and scattered biotite-clots. Similarly, megacrysts and disrupted sheets of coarse-grained granite are dispersed inside diatexite, which now has variable colours, reflecting different modal contents, and heterogeneous grainsizes (Fig. 8c). Such zones are typically related to domains of more intense deformation with significant stretching of former magma sheets (Fig. 8d).

3.2.4. Leucogranite and pegmatite dikes

Multiple generations of leucogranites and pegmatite dikes and sills cut across the migmatite. Like the megacrystic granites, these intrusions display various types of contacts with the diatexite (Fig. 9). Early dikes vary from irregular, disrupted and folded sections, to strongly disaggregated intrusions broken down to individual grains (Fig. 9a–b). Late intrusions form planar dikes with sharp curved contacts and variable widths (Fig. 9c, N–S oriented dike). In between these extremes are dikes with contorted geometries that have irregular, lobated or crenulated contacts with diatexites (Fig. 9c, E–W oriented dike).

3.3. Deformation

Weinberg et al. (2013) recognized four syn-anatectic deformation phases towards the east of the area covered here. In their work D1 and D2 are compressional deformation phases with melt migration along fold limbs and axial planar dikes. D3 and D4 are transtensional events with dextral shearing, melt accumulation and formation of diatexites. At Stun'Sail Boom, evidence for the early deformation phases

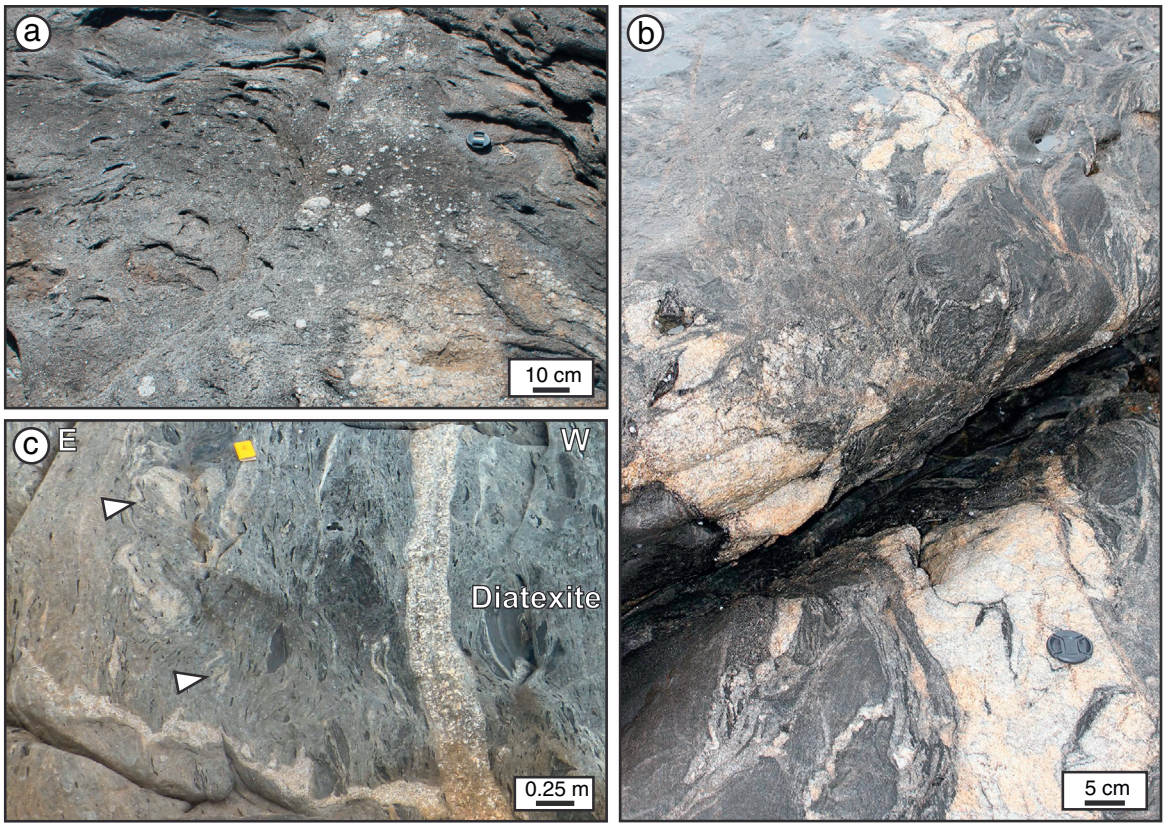

Fig. 9. Different generations of leucogranite dikes intruding diatexite. (a) Coarse leucogranite at the base of the photograph grades upwards into a wedge-shaped band of diatexite with dispersed megacrysts of K-feldspar and quartz, suggesting disaggregation of the leucogranite. (b) Leucogranite dike disrupted into isolated blocks with irregular, folded contacts, forming a trail in diatexite. (c) Steep outcrop surface showing two generations of leucogranite intruding diatexite. An E–W trending leucogranite dike, intruded at high angles to dominant magmatic foliation, has strongly irregular contacts indicating partially molten surroundings. Small patches of leucogranite in the diatexite disconnected from the dike (white arrows) point to possible disaggregation during intrusion. This dike is crosscut by a late, N–S trending, coarse-grained leucogranite with sharp and more planar contacts sub-parallel to the foliation in the diatexite.

is only preserved in metatexite and large schollen in diatexite where bedding records centimetre-scale, isoclinal folding and mesoscale, upright folding. Foliations related to these events have been exploited as melt migration pathways and are marked by networks that connect layer-parallel with axial-planar leucosomes (Fig. 2b). These features correlate to the early syn-anatectic upright folding D2 event in Weinberg et al., 2013. In Stun'Sail Boom however, a syn-magmatic thrusting event overprints most of the earlier events and correlates to their D4.

This dominant deformation phase is characterized by two main foliations in diatexites. Both are NW-dipping and defined by the asymmetric organization of schollen and schlieren (Fig. 10a–b). The steeper plane with average dips of 50°NW comprises schollen rich areas. The foliation, as well as schollen tips and schlieren rotate into planes with average dips of 30°NW, comprising magma-rich diatexite with few schollen and schlieren. This pattern represents a thrust duplex, where S-planes are dragged into the gently dipping shear planes and result in sigma-shaped schollen, with an asymmetry indicative of top-to-ESE shearing. A stretching lineation related to thrusting could not be identified, but folded leucosomes in metatexite have fold axes with plunges close to the down-dip direction of the shear planes (30–40° towards 310°) and are interpreted to be parallel to the transport direction during thrusting (Fig. 10c and stereonet inset). We note that planes perpendicular to this direction show a systematic asymmetry in the arrangement of schollen and schlieren, suggesting an additional dextral component during thrusting.

Despite the mesoscale evidence for thrusting, diatexites are weakly deformed at the microscale. Igneous textures such as euhedral plagioclase and interstitial quartz grains dominate, and indicators for sub-solidus deformation are limited to chessboard extinction of quartz (Fig. 10d). These features imply that deformation and flow of diatexite took place in the magmatic state, followed by weak straining after magma solidification (Sawyer, 1998; Weinberg et al., 2013). We conclude that strain was preferentially accommodated by flow along melt-rich shear planes, preventing solid-state deformation and development of a strong mineral lineation.

4. Discussion

4.1. Magma hybridization

We interpret the contacts depicted in Figs. 5–9 to represent different stages of magma hybridization between *in source* anatectic magmas and external magmas, in a multi-step process. As recognized by Foden et al. (2002), irregular and interfingering contacts suggest that megacrystic granite and diatexite were magmas when they interacted. Mingling resulted in material transfer from one magma to the other: K-feldspar megacrysts were transferred to the diatexite, while megacrystic granites gained schlieren and schollen from the diatexite. The intensity of hybridization varies from almost none in the "sheeted zone" where only a few, isolated grains or schollen were transferred across well-defined contacts (Fig. 6d), to disruption of the sheets in the "lensed zones", to the development of strongly hybridized magmas sharing characteristics of both end-members in the "heterogeneous zone" (Fig. 8c).

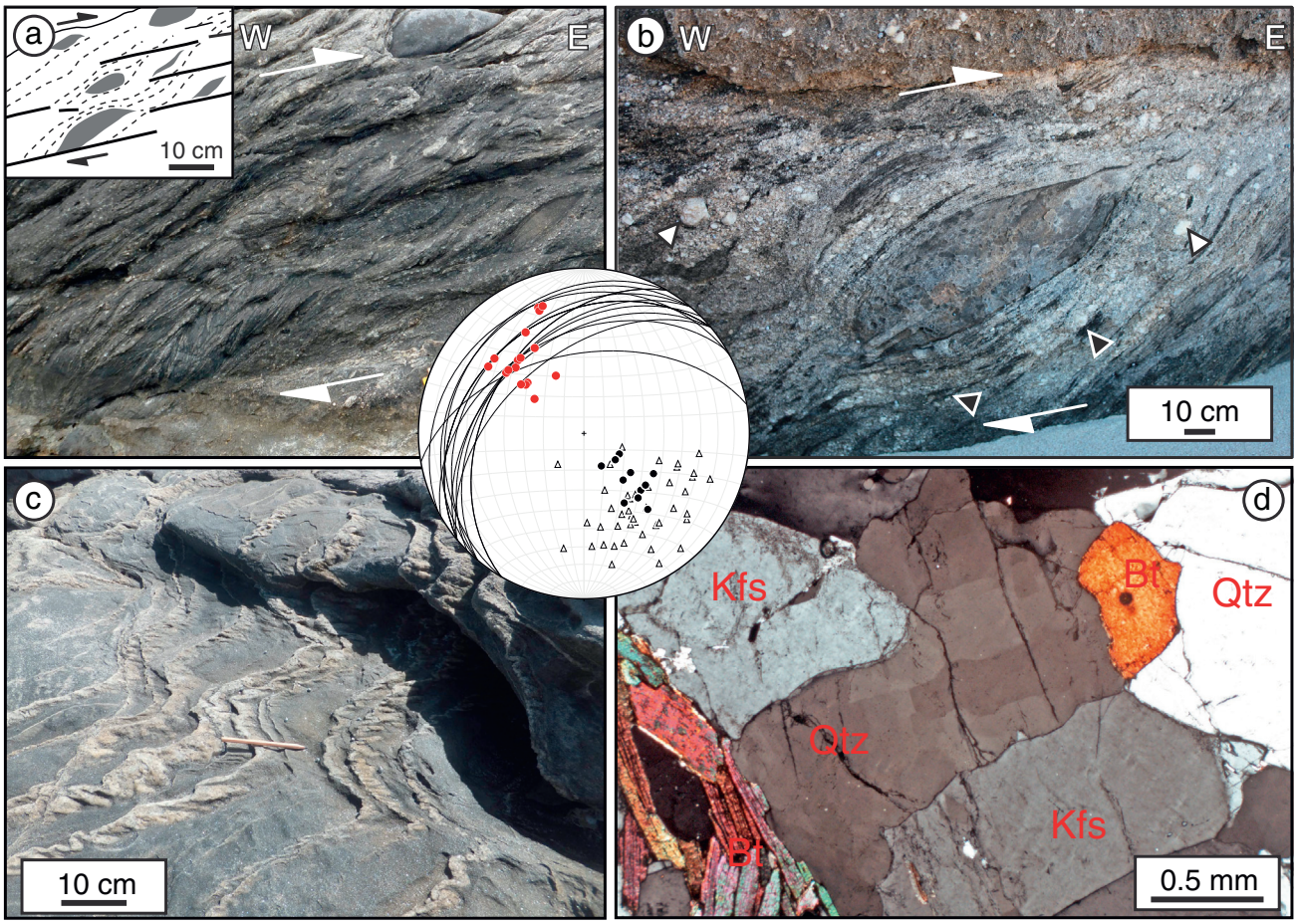

Fig. 10. Syn-magmatic thrusting. (a, b) Top-to-E thrusting of diatexite marked by asymmetric arrangement or sigmoidal schollen and melt-rich sheets on a vertical exposure, defining a mesoscale duplex. Shear bands have average dips of 30° NW. The diatexite in (b) is a hybrid with Kfs-megacrysts (white arrows) and disaggregated biotite-clots and schlieren (black arrows). (c) Folded leucosomes in metatexite. Fold axes have consistent NW-plunge, close to down dip of shear plane, suggesting development related to the shearing. (d) Photomicrograph of diatexite showing weak sub-solidus deformation, marked by high-T chessboard extinction in quartz (cross-polarized light). Inset is a lower-hemisphere projection, equal area stereonet showing orientation of C-planes as great circles and poles (black dots, n = 22) and leucosome fold axes, interpreted to represent the transport direction (red circles n = 14). Open triangles represent poles to the steeper S-planes (n = 47). (For interpretation of the references to colour in this figure legend, the reader is referred to the web version of this article.)

Advanced hybridization stages are best developed in zones of intense deformation, suggesting a key role for deformation in mixing and magma distribution on Kangaroo Island. Active shearing generates low pressure planes that attract and channel fluids and magmas (Mancktelow, 2006), thus providing preferential magma pathways (Brown and Solar, 1998; Reichardt et al., 2010; Weinberg et al., 2009). The outcrops described here show a similar behaviour. Gently dipping shear planes attracted melt from the schollen-rich diatexite domains in between (Fig. 10). Furthermore, the existence of hybridized magmas in the same planes (Fig. 8d) indicates intrusive magmas flowed along the same pathways in response to a combination of tectonic and buoyancy stresses. The presence of solids of varied shapes and sizes in both magmas created flow perturbations that maximized the stretching and folding of magmas that led to mingling (Figs. 6–9, Perugini and Poli, 2012; Ubide et al., 2014). Continued flow gradually equalized rheological and physical properties making mixing increasingly easier.

Contact relationships between leucogranite dikes and diatexite allow us to differentiate between several intrusion phases (Figs. 5, 9): (i) early intrusions were crystallized and disaggregated into angular blocks and individual isolated crystals as the melt fraction in the surroundings gradually increased and reached a critical proportion to allow bulk flow (Fig. 9a); (ii) intrusions contemporaneous with peak anatexis interacted with diatexite and formed irregularly folded and disrupted trails of leucogranite blocks (Fig. 9b and E–W oriented dike in Fig. 9c); (iii) late intrusions that intruded close to the solidus of the wall rock remained reasonably continuous and planar, with variable widths and curved contacts with only minor hybridization (Fig. 9c, N–S oriented dike).

Further to the process of hybridization with local magmas, we have recognized that two very similar megacrystic granites intruded the current exposure levels. The contacts between the two range from sharp and truncating, including composite enclaves of gneissic granite in the intrusive megacrystic granite (Fig. 4); to diffuse and interfingering contacts, suggesting that in some sections the younger megacrystic granite intruded the gneissic granite while this was still a mush. These features are identical to the intrapluton erosion and recycling described in Paterson et al. (2016) and indicate that several intrusive batches reached this anatectic zone and interacted amongst themselves.

In summary, the variety of hybridization features results from the combination of multiple intrusion into an anatectic zone and contemporaneous magma flow during deformation. This is consistent with a long anatectic history of up to 30 m yr recorded by monazite (495–465 Ma, Weinberg et al., 2013). During this time, different sections may have reached maximum melt fraction at different stages resulting in varying styles of interaction and distinct degrees of mingling with intrusive

magmas. The efficiency of hybridization in this environment is a function of many variables such as the physical state of the two magmas, the nature of flow resulting from new magma intrusions and pressure gradients imposed by gravity, external stresses and the evolving geometry.

4.2. Origin of magmas

Foden et al. (2002) characterized the different magmatic rocks on Kangaroo Island based on their geochemistry and showed that the Kanmantoo Group is an important constituent of both the intrusive granite and local diatexite. The intrusive granites have been derived from unexposed, lower regions as a result of different degrees of interaction with hot mafic magmas. In contrast, the diatexites are *in source* products of crustal melting. Regional P–T estimates from earlier studies describe the Adelaide Fold Belt as a typical low-pressure/high-temperature orogen with pressures below 4.5 kbar (Alias et al., 2002; Dymoke and Sandiford, 1992). A minimum pressure for the migmatites can be estimated from the intrusive muscovite-rich leucogranites (Fig. 3d), which are considered as segregated and fractionated crustal melts (Foden et al., 2002). Primary muscovite in leucogranites commonly crystallizes close to the solidus in peraluminous magmas, but requires pressures above 3.5 kbar (*e.g.* Scaillet et al., 2016).

A minimum temperature has been constrained by the presence of peritectic sillimanite in the migmatites, regarded to represent muscovite dehydration melting (Tassone, 2008), which takes place between 680 and 740 °C, depending on pressure. This is consistent with the stable appearance of biotite and the absence of ferromagnesian peritectic minerals, implying that temperature did not reach biotite dehydration conditions, typically at T > 750 °C. However, sillimanite in migmatites is rare and only occurs in a few pelite layers as fine needles included in skeletal, late-formed muscovite, therefore raising questions about the importance of this reaction.

Most of the exposed unmelted Kanmantoo Group in the northern side of the island is poor in muscovite (<5 vol.%), which explains the variable but low modal proportion of either muscovite or sillimanite in the migmatites, and suggests that breakdown of muscovite would have been a limiting factor in melt production. In addition, peritectic K-feldspar, another product of muscovite dehydration, is sparse or absent in most residual layers. For these reasons, dehydration melting only cannot explain the high melt volumes necessary to form diatexites.

We argue that melting was assisted by the influx and heterogeneous distribution of H_2O-rich fluids (Weinberg and Hasalová, 2015; White et al., 2005). This is demonstrated by a simple mass balance. Assuming average muscovite contains 4 wt.% H_2O bound in the crystal structure, and an upper bound of 5 wt.% muscovite presents throughout the protolith, then the effective H_2O budget in the rock is 0.2 wt.%. At estimated metamorphic conditions of 680–740 °C and 4–5 kbar, a granitic melt requires 5–9.5 wt.% H_2O to be stabilized (Johannes and Holtz, 1996). It follows that only ~2–4% of melt could be produced if muscovite was the only source of water. We therefore suggest that melting occurred *via* a combination of melting reactions ranging from muscovite dehydration:

$$Ms + Qtz + Pl = Melt + Kfs + Sil + Bt \quad (1)$$

(Patiño Douce and Harris, 1998)

responsible for small melt volumes, assisted by melting in the presence of H_2O-rich fluid, such as:

$$Ms + Pl + Qtz + H_2O = Melt \quad (2)$$

(Patiño Douce and Harris, 1998)

or

$$Qtz + Pl + Kfs + H_2O = Melt \quad (3)$$

(Sawyer, 1998, minerals abbreviation after Kretz, 1983)

We note however, that rock disaggregation and formation of diatexites are likely a combined result of melt produced *in situ* and internal migration of melt within the source. The common existence of diatexite in areas rich in injected granite also suggests a genetic relationship with intrusion, such as the addition of heat and fluids to the protoliths.

4.3. Source of water — multiple intrusions of granite magmas

The relationships between granite intrusions and surrounding migmatite formation in the Adelaide Fold Belt have been ascribed to advective heat transfer from the external magmas (Foden et al., 2002; Sandiford et al., 1992; Sandiford et al., 1995). An additional role of these felsic intrusions as a carrier of H_2O has not been considered, although water-fluxed melting has been proposed to explain large magma volumes in parts of the orogen (Cartwright et al., 1995).

During prograde metamorphism any water that exists in excess to the saturation of hydrous phases in a rock is consumed at the wet solidus, where melting buffers the temperature until exhaustion of at least one of the reactants (*e.g.* typically H_2O). Provided appropriate conditions, it is possible to introduce fluids into suprasolidus crust and prevent H_2O from being consumed at the solidus isotherm. There are several possibilities to overcome this natural barrier and to transport fluids into the core of hot, anatectic terranes (Weinberg and Hasalová, 2015). One way is to concentrate fluids in efficient channels, such as shear zones or fracture systems, allowing the direct influx of water into the hot terrane (Sawyer, 2010). Another option is the intrusion and crystallization of water-rich magmas from deeper levels. The potential of crustal felsic magmas to heat the crust is lower than for basaltic magmas, but they can carry large volumes of dissolved H_2O. Upon decompression or crystallization, these granitic magmas expel water to their surrounding where they may cause extensive melting if surrounding temperatures are above the water-saturated solidus (Finger and Clemens, 1995; Holk and Taylor, 2000). Likewise, chemical potential gradients develop due to different water activities in water-rich intrusions and their water-poor surrounding that can drive H_2O diffusion (White and Powell, 2010). Weinberg and Hasalová (2015) hypothesized that the ingress of a water-rich magma into a hot terrane with a lower water activity could cause development of an anatectic front around the intrusions, as water diffuses to equalize these potential gradients.

On Kangaroo Island all the mechanisms might combine during a progressive evolution. We consider that the outcrops record processes in a hot section of the crust which was a passageway of deeper crustal granite magmas that interacted with mafic magmas (Foden et al., 2002). These intrusive magmas advected both heat and H_2O, triggering profuse melting by reactions (2) and (3). Possible evidence for early stages of this process are shown in Fig. 11 where granite surrounds and intrudes turbidite schollen that melted at their contact, forming a leucocratic, fine-grained granitic phase, identical to those interpreted to be derived from anatexis in metatexite.

Early intrusions would have been unable to mingle with local magmas, however they contributed to a step-wise increase in the local melt fraction, by raising the heat and water budget of the system (Fig. 12). Over extended time and multiple intrusions, the system became hotter and wetter, forming a mushy diatexite that impeded new intrusions to traverse the area. These were temporarily trapped in this zone, leading to a more efficient thermal and chemical equilibration with the surroundings and creating opportunities for mixing as diatexite and intrusive magmas flowed together due to imposed deformation (Fig. 12, top right inset). Over the duration of the anatectic

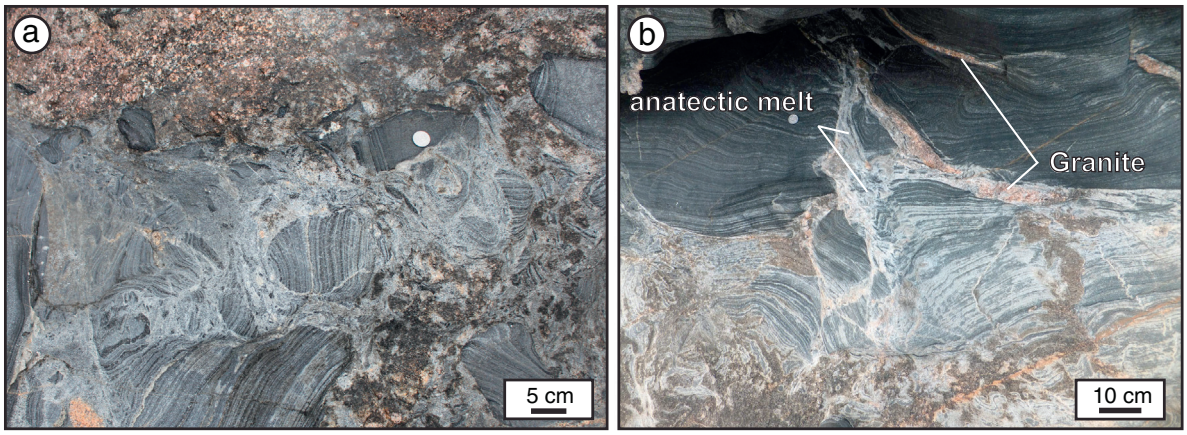

Fig. 11. Intrusive magma as possible melting agent. (a) Irregular contact between coarse-grained megacrystic granite and fine-grained grey granite, packed with rotated schollen. (b) Large, layered and dominantly unmelted psammite schollen surrounded by megacrystic granite and disrupted into blocks separated by narrow stringers of grey anatectic granite. In both photographs the fine-grained granite is similar to leucosomes in metatexite (compare to Fig. 2b), suggesting that they are *in situ* melts.

event, external magmas flowed in, became trapped, partly homogenized and then flowed out again. Whether magmas flowed in or out of the region is controlled by both the evolving tectonic pressure gradients and the buoyancy of the magmas.

In such a system, the total melt fraction at any point in time and space depends on the changing distribution of heat and H_2O, which may have been highly variable. It is this net balance between inflow and outflow of heat and H_2O that controls the long-term existence of this mixing zone. As long as heat and fluid advection is maintained by magma intrusion, water-fluxed melting will take place and temperatures will be buffered by melting. A decrease in the advection of heat and fluids, caused by changes such as regional exhumation or decreased influx of mantle heat, will lead to the end of the melting and hybridization process. Late intrusions that crosscut the hybrid magmatic rocks and migmatites mark these final stages. Volatiles exsolved from these late magmas may have caused retrogression, explaining the generation of irregular shaped, retrograde muscovite formed after K-feldspar and sillimanite (Type 2 muscovite in migmatites; Solar and Brown, 2001).

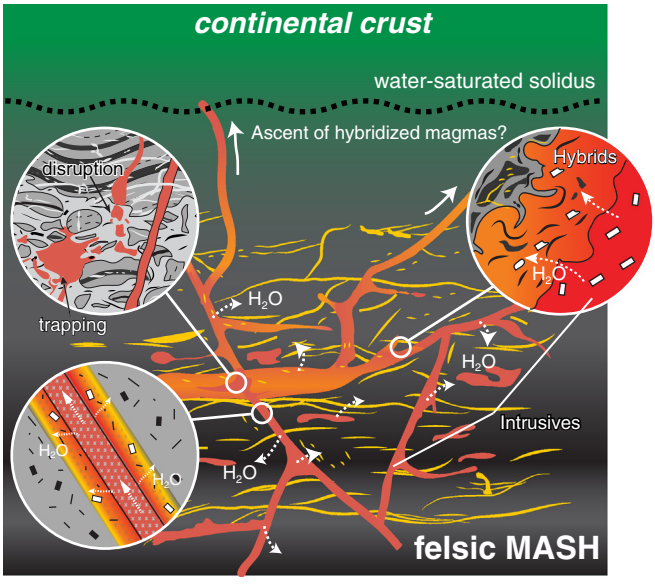

Fig. 12. Magmatic processes giving rise to a felsic MASH region analogous to processes envisaged by Hildreth and Moorbath (1988) for magmatic arc roots. The difference here is that instead of juvenile magmas, the melting agent is the intrusive crustal, granitic magma carrying heat and H_2O (lower left inset) creating a low viscosity environment where new intrusions are trapped and reinforce *in situ* melting. This gives rise to a region where magmas are stored and homogenized (top insets). Early intrusions become disaggregated in this felsic MASH zone. As the system cools, late dikes are discordant to earlier structures (top left inset). Bottom left inset adapted from Weinberg and Hasalová (2015).

4.4. Felsic MASH and granite variety

Traditionally magma mixing is associated with the very different felsic crustal and mafic mantle magmas. Instead, we envisage mixing as a multiple step interaction between any variety of magmas that may take place several times and anywhere in a granitic system, from its roots to the emplacement levels in plutons. Though less obvious in the field, magmas of similar composition are more easily mixed. For example, a felsic granitic magma can readily mix with other granitic magmas derived from different sources and varied melting reactions, or with evolved magmas derived from the fractionation of mantle magmas, creating complex magma suites. Similar processes have been described in the Tynong Province in southeastern Australia by Regmi et al. (2016), and in the Karakoram Ranges where Reichardt et al. (2010) reported hybridization between different crustal melts along their pathways to plutons. The latter is consistent with studies that show the redistribution or local storage of magma pulses within the hot crust before final ascent, allowing periods of felsic magma interaction near their sources (Diener et al., 2014; Hall and Kisters, 2016).

The self-reinforcing process between trapping of intrusive granites and crustal melting described above, created zones of magma generation, storage and mixing within the anatectic continental crust. This comprises all the ingredients included in the original MASH zone hypothesis of Hildreth and Moorbath (1988). We conclude that Kangaroo Island migmatites record a felsic MASH zone that differs from the original in that it was neither at the base of an arc nor formed by a direct contribution of mantle magmas (Fig. 12).

There are four aspects of the rock record on Kangaroo Island that add to the original MASH model: (a) a positive feedback between granite intrusion and formation of a MASH zone through *in situ* melting, (b) a significant role for the transfer of aqueous fluids, analogous to the "deep crustal hot zone" model of Annen et al. (2006), (c) the role of deformation in assisting hybridization, and finally, (d) felsic MASH zones can develop in a variety of tectonic settings, not only magmatic arcs, without the requirement of direct mantle contribution. In our modified felsic MASH zone the difficulties in mixing felsic and mafic magmas (Sparks and Marshall, 1986) are alleviated in a number of ways: (a) intrusive granite magmas are trapped at conditions above their solidus and therefore can hybridize more efficiently with their partially molten surroundings, (b) deformation assists magma hybridization by forcing flow, and (c) magmas have similar physical properties (*e.g.* densities and viscosities).

The outcrops described here demonstrate the significance of water-fluxed melting and magma mixing in the evolution of the crust through creating propitious feedback processes that generate felsic MASH zones and controlling the origin of granites. The melt production exposed at Kangaroo Island is likely to be magnitudes smaller than their deep crustal counterparts driven by input of mafic magmas. It is not clear how much and how far the hybridized magmas generated in the exposed felsic MASH zone migrated to higher structural positions, but Weinberg et al. (2013) pointed to several deformation-driven melt extraction mechanisms, suggesting that some of the magma may have been extracted. In addition, there are a number of crustal-derived plutons that have intruded shallower levels of the Adelaide Fold Belt (Alias et al., 2002).

Moreover, the recognition that granite magma ascent in the crust evolves through multiple stages, with periods of intra-crustal magma interaction in felsic MASH zones, contributes to a better understanding of granite evolution. Identification of a hybrid origin of single intrusions in the assemblage of plutons is not straightforward and evidence might be masked by homogenization, but the possibility of hybridization intervals before final emplacement should be considered, in particular when interpreting irregular geochemical, geochronological or isotope data. Following the traditional scale-independence of geological processes, we argue that the small-scale features described on Kangaroo Island reflect large-scale mechanisms controlling the global complexity of granite belts.

5. Conclusion

The south coast of Kangaroo Island has migmatites formed through muscovite dehydration melting assisted by water-fluxed melting of the Kanmantoo Formation turbidites at pressures between 3.5 and 4.5 kbar. We suggest that multiple intrusions of external granitic magmas brought in H_2O and heat leading to a gradual increase in melt fraction. Syn-magmatic deformation in this anatectic zone enhanced mingling and mixing between intrusive and local crustal magmas and led to the variety of exposed granitoids. Moreover, with a gradually increasing melt fraction, new intrusions became trapped and gave rise to a positive feedback between intrusion and *in situ* melting with increased mixing opportunities. This feedback gave rise to a long-lasting felsic zone of melting, assimilation, storage and homogenization: a felsic MASH zone. Any magma escaping a felsic MASH zone as described may have a homogeneity that hides a complex multi-step history. The outcrops at Kangaroo Island show how such a MASH zone can develop away from arcs, in pure crustal environments, where fluid transfer from felsic magma intrusions play a crucial role in the evolution of the system.

Acknowledgements

This work was financially supported by ARC DP11010254. We would like to thank M. Richter and N. Rivett for their assistance during field work. F. Clos and C. Wilson are thanked for reviewing an earlier version of the manuscript. In addition we would like to thank Bob Wiebe and Johann Diener for their constructive reviews, which much improved the manuscript.

Appendix A. Supplementary data

Supplementary data associated with this article can be found in the online version, at doi: 10.1016/j.lithos.2017.03.030. These data include the Google map of the field areas described in this article.

References

Alias, G., Sandiford, M., Hand, M., Worley, B., 2002. The P-T record of synchronous magmatism, metamorphism and deformation at Petrel Cove, southern Adelaide Fold Belt. Journal of Metamorphic Geology 20, 351–363.

Annen, C., Blundy, J.D., Sparks, R.S.J., 2006. The genesis of intermediate and silicic magmas in deep crustal hot zones. Journal of Petrology 47, 505–539.

Brown, M., 2013. Granite: from genesis to emplacement. Geological Society of America Bulletin 125, 1079–1113.

Brown, M., Solar, G.S., 1998. Shear-zone systems and melts: feedback relations and self-organization in orogenic belts. Journal of Structural Geology 20, 211–227.

Cartwright, I., Vry, J., Sandiford, M., 1995. Changes in stable isotope ratios of metapelites and marbles during regional metamorphism, Mount Lofty Ranges, South Australia: implications for crustal scale fluid flow. Contributions to Mineralogy and Petrology 120, 292–310.

Carvalho, B.B., Sawyer, E.W., Janasi, V.A., 2016. Crustal reworking in a shear zone: transformation of metagranite to migmatite. Journal of Metamorphic Geology 34, 237–264.

Chappel, B.W., White, A.J.R., Wyborn, D., 1987. The importance of residual source material (restite) in granite petrogenesis. Journal of Petrology 28, 1111–1138.

Clemens, J.D., Stevens, G., 2012. What controls chemical variation in granitic magmas? Lithos 134–135, 317–329.

Clemens, J.D., Stevens, G., 2016. Melt segregation and magma interactions during crustal melting: breaking out of the matrix. Earth Science Reviews 160, 333–349.

Collins, W.J., 1996. Lachlan Fold Belt granitoids: products of three-component mixing. Geological Society of America Special Papers 315, 171–181.

Collins, W.J., Huang, H.Q., Jiang, X.Y., 2016. Water-fluxedcrustal melting produces Cordilleran batholiths. Geology 44, 143–146.

Diener, J.F.A., White, R.W., Hudson, T.J.M., 2014. Melt production, redistribution and accumulation in mid-crustal source rocks, with implications for crustal-scale melt transfer. Lithos 200–201, 212–225.

Dymoke, P., Sandiford, M., 1992. Phase relationships in Buchan facies series pelitic assemblages: calculations with application to andalusite-staurolite parageneses in the Mount Lofty Ranges, South Australia. Contributions to Mineralogy and Petrology 110, 121–132.

Fanning, C.M., 1990. Single grain dating of a granite sample from Cape Willoughby, Kangaroo Island, Prise Laboratories, Australian National University Progress Report: 089-060. South Australia, Department of Mines and Energy, Open File Envelope 8828, pp. 29–32.

Farina, F., Dini, A., Rocchi, S., Stevens, G., 2014. Extreme mineral-scale Sr isotope heterogeneity in granites by disequilibrium melting of the crust. Earth and Planetary Science Letters 399, 103–115.

Finger, F., Clemens, J.D., 1995. Migmatization and "secondary" granitic magmas: effects of emplacement and crystallization of "primary" granitoids in Southern Bohemia, Austria. Contributions to Mineralogy and Petrology 120, 311–326.

Flöttmann, T., Haines, P., Jago, J., James, P., Belperio, A., Gum, J., 1998. Formation and reactivation of the Cambrian Kanmantoo Trough, SE Australia: implications for early Palaeozoic tectonics at eastern Gondwana's plate margin. Journal of the Geological Society 155, 525–539.

Foden, J.D., Turner, S., Morrison, R., 1990. Tectonic implications of Delamerian magmatism in South Australia and western Victoria. In: Jago, J.B., Moore, P.S. (Eds.), The Evolution of a Late Precambrian-Early Palaeozoic Rift Complex: The Adelaide Geosyncline. Geological Society of Australia; Special Publication, pp. 465–482.

Foden, J.D., Sandiford, M., Dougherty-Page, J., Williams, I., 1999. Geochemistry and geochronology of the Rathjen Gneiss: implications for the early tectonic evolution of the Delamerian Orogen. Australian Journal of Earth Sciences 46, 377–389.

Foden, J.D., Elburg, M.A., Turner, S.P., Sandiford, M., O'Callaghan, J., Mitchell, S., 2002. Granite production in the Delamerian Orogen, South Australia. Journal of the Geological Society 159, 557–575.

Foden, J.D., Elburg, M.A., Dougherty-Page, J., Burtt, A., 2006. The timing and duration of the Delamerian orogeny: correlation with the Ross Orogen and implications for Gondwana assembly. Journal of Geology 114, 189–210.

Gray, C.M., Kemp, A.I.S., 2009. The two-component model for the genesis of granitic rocks in southeastern Australia — nature of the metasedimentary-derived and basaltic end members. Lithos 111, 113–124.

Hall, D., Kisters, A., 2016. Episodic granite accumulation and extraction from the mid-crust. Journal of Metamorphic Geology 34, 483–500.

Hasalova, P., Weinberg, R.F., Macrae, C., 2011. Microstructural evidence for magma confluence and reusage of magma pathways: implications for magma hybridization, Karakoram Shear Zone in NW India. Journal of Metamorphic Geology 29, 875–900.

Hildreth, W., Moorbath, S., 1988. Crustal contributions to arc magmatism in the Andes of Central Chile. Contributions to Mineralogy and Petrology 98, 455–489.

Holk, G.J., Taylor, H.P., 2000. Water as a petrologic catalyst driving $^{18}O/^{16}O$ homogenization and anatexis of the middle crust in the metamorphic core complexes of British Columbia. International Geology Review 42, 97–130.

Jenkins, R.J.F., Cooper, J.A., Compston, W., 2002. Age and biostratigraphy of early Cambrian tuffs from SE Australia and southern China. Journal of the Geological Society 159, 645–658.

Johannes, W., Holtz, F., 1996. Petrogenesis and Experimental Petrology of Granitic Rocks. Springer, Berlin, New York.

Keay, S., Collins, W.J., McCulloch, M.T., 1997. A three-component Sr-Nd isotopic mixing model for granitoid genesis, Lachlan fold belt, eastern Australia. Geology 25, 307–310.

Kretz, R., 1983. Symbols for rock-forming minerals. American Mineralogist 68, 277–279.

Mancktelow, N.S., 1990. The structure of the southern Adelaide Fold Belt, South Australia. In: Jago, J.B., Moore, P.S. (Eds.), The Evolution of a Late Precambrian-Early Palaeozoic Rift Complex: The Adelaide Geosyncline. Geological Society of Australia; Special Publication, pp. 369–395.

Mancktelow, N.S., 2006. How ductile are ductile shear zones? Geology 34, 345–348.

Paterson, S., Memeti, V., Mundil, R., Žák, J., 2016. Repeated, multiscale, magmatic erosion and recycling in an upper-crustal pluton: Implications for magma chamber dynamics and magma volume estimates. American Mineralogist 101, 2176–2198.

Patiño Douce, A.E., Harris, N., 1998. Experimental constraints on Himalayan anatexis. Journal of Petrology 39, 689–710.
Patiño Douce, A.E., Johnston, A.D., 1991. Phase equilibria and melt productivity in the pelitic system: implications for the origin of peraluminous granitoids and aluminous granulites. Contributions to Mineralogy and Petrology 107, 202–218.
Perugini, D., Poli, G., 2012. The mixing of magmas in plutonic and volcanic environments: analogies and differences. Lithos 153, 261–277.
Regmi, K.R., Weinberg, R.F., Nicholls, I.A., Maas, R., Raveggi, M., 2016. Evidence for hybridization in the Tynong Province granitoids, Lachlan Fold Belt, eastern Australia. Australian Journal of Earth Sciences 1–21.
Reichardt, H., Weinberg, R.F., 2012a. The dike swarm of the Karakoram shear zone, Ladakh, NW India: linking granite source to batholith. Geological Society of America Bulletin 124, 89–103.
Reichardt, H., Weinberg, R.F., 2012b. Hornblende Chemistry in Meta- and Diatexites and its Retention in the Source of Leucogranites: an Example from the Karakoram Shear Zone, NW India. Journal of Petrology 53, 1287–1318.
Reichardt, H., Weinberg, R.F., Andersson, U.B., Fanning, C.M., 2010. Hybridization of granitic magmas in the source: the origin of the Karakoram Batholith, Ladakh, NW India. Lithos 116, 249–272.
Sandiford, M., Foden, J.D., Shaohua, Z., Turner, S., 1992. Granite genesis and the mechanics of convergent orogenic belts with application to the southern Adelaide Fold Belt. Transactions of the Royal Society of Edinburgh: Earth Sciences 83, 83–93.
Sandiford, M., Eraser, G., Arnold, J., Foden, J.D., Farrow, T., 1995. Some causes and consequences of high-temperature, low-pressure metamorphism in the eastern Mt Lofty Ranges, South Australia. Australian Journal of Earth Sciences 42, 233–240.
Sawyer, E.W., 1998. Formation and evolution of granite magmas during crustal reworking: the dignificance of diatexites. Journal of Petrology 39, 1147–1167.
Sawyer, E.W., 2010. Migmatites formed by water-fluxed partial melting of a leucogranodiorite protolith: microstructures in the residual rocks and source of the fluid. Lithos 116, 273–286.
Sawyer, E.W., Cesare, B., Brown, M., 2011. When the continental crust melts. Elements 7, 229–234.
Scaillet, B., Holtz, F., Pichavant, M., 2016. Experimental constraints on the formation of silicic magmas. Elements 12, 109–114.
Solar, G.S., Brown, M., 2001. Petrogenesis of migmatites in Maine, USA: possible source of peraluminous leucogranite in plutons? Journal of Petrology 42, 789–823.
Sparks, R.S.J., Marshall, L.A., 1986. Thermal and mechanical constraints on mixing between mafic and silicic magmas. Journal of Volcanology and Geothermal Research 29, 99–124.
Stevens, G., Clemens, J.D., Droop, G.T.R., 1997. Melt production during granulite-facies anatexis: experimental data from “primitive” metasedimentary protoliths. Contributions to Mineralogy and Petrology 128, 352–370.
Stevens, G., Villaros, A., Moyen, J., 2007. Selective peritectic garnet entrainment as the origin of geochemical diversity in S-type granites. Geology 35, 9–12.
Tassone, D.R., 2008. Crustal Melting and Melt Extraction: The Role of Migmatites in the Evolution of the Southern Adelaide Fold-Thrust Belt. (Honours Thesis). The University of Adelaide, Adelaide, p. 107.
Turner, S., Haines, P., Foster, D., Powell, R., Sandiford, M., Offler, R., 2009. Did the Delamerian orogeny start in the Neoproterozoic? The Journal of Geology 117, 575–583.
Ubide, T., Galé, C., Larrea, P., Arranz, E., Lago, M., Tierz, P., 2014. The relevance of crystal transfer to magma mixing: a case study in composite dykes from the Central Pyrenees. Journal of Petrology 55, 1535–1559.
Vanderhaeghe, O., 2001. Melt segragation, pervasive melt migration and magma mobility in the continental crust: the structural record from pores to orogens. Physics and Chemistry of the Earth, Part A: Solid Earth and Geodesy 26, 213–223.
Waight, T.E., Maas, R., Nicholls, I.A., 2000. Fingerprinting feldspar phenocrysts using crystal isotopic composition stratigraphy: implications for crystal transfer and magma mingling in S-type granites. Contributions to Mineralogy and Petrology 139, 227–239.
Weber, C., Barbey, P., 1986. The role of water, mixing processes and metamorphic fabric in the genesis of the Baume migmatites (Ardèche, France). Contributions to Mineralogy and Petrology 92, 481–491.
Weinberg, R.F., Hasalová, P., 2015. Water-fluxed melting of the continental crust: a review. Lithos 212–215, 158–188.
Weinberg, R.F., Regenauer-Lieb, K., 2010. Ductile fractures and magma migration from source. Geology 38, 363–366.
Weinberg, R.F., Mark, G., Reichardt, H., 2009. Magma ponding in the Karakoram shear zone, Ladakh, NW India. Geological Society of America Bulletin 121, 278–285.
Weinberg, R.F., Hasalová, P., Ward, L.K., Fanning, C.M., 2013. Interaction between deformation and magma extraction in migmatites: examples from Kangaroo Island, South Australia. Geological Society of America Bulletin 125, 1282–1300.
White, R.W., Powell, R., 2010. Retrograde melt–residue interaction and the formation of near-anhydrous leucosomes in migmatites. Journal of Metamorphic Geology 28, 579–597.
White, R.W., Pomroy, N.E., Powell, R., 2005. An in situ metatexite–diatexite transition in upper amphibolite facies rocks from Broken Hill, Australia. Journal of Metamorphic Geology 23, 579–602.
Yakymchuk, C., Brown, M., 2014. Consequences of open-system melting in tectonics. Journal of the Geological Society 171, 21–40.